EMD/HT-based local fault detection in DC microgrid clusters

Bayati, Navid; Baghaee, Hamid Reza; Savaghebi, Mehdi; Hajizadeh, Amin; Soltani, Mohsen; Lin, Zhengyu

Published in:
IET Smart Grid

DOI (link to publication from Publisher):
10.1049/stg2.12060

Publication date:
2022

Document Version
Publisher's PDF, also known as Version of record

Received: 18 November 2021 | Revised: 31 January 2022 | Accepted: 12 February 2022

DOI: 10.1049/stg2.12060

IET Smart Grid

The Institution of Engineering and Technology WILEY

ORIGINAL RESEARCH

EMD/HT-based local fault detection in DC microgrid clusters

Navid Bayati[1] | Hamid Reza Baghaee[2] | Mehdi Savaghebi[1] | Amin Hajizadeh[3] | Mohsen Soltani[3] | Zhengyu Lin[4]

[1]Department of Mechanical and Electrical Engineering, University of Southern Denmark, Odense, Denmark

[2]Department of Electrical Engineering, Amirkabir University of Technology, Tehran, Iran

[3]Department of Energy, Aalborg University, Aalborg, Denmark

[4]Wolfson School of Mechanical, Electrical and Manufacturing Engineering, Loughborough University, Loughborough, UK

Correspondence

Navid Bayati, Department of Mechanical and Electrical Engineering, University of Southern Denmark, Odense, Denmark.
Email: navib@sdu.dk

Abstract

DC faults can create serious damages if not detected and isolated in a short time. This paper proposes a fault detection technique for DC faults to enhance the protection of DC microgrid clusters. To detect such faults accurately and quickly, a DC fault detection scheme using empirical mode decomposition and Hilbert transform is proposed. Due to the strict time limits for fault interruption caused by fast high-rising fault currents in DC systems, DC microgrid clusters' protection remains a challenging task. Furthermore, high impedance faults (HIFs) in DC systems cause a small change in the current, which can damage the power electronic converters if not detected in time. Therefore, this paper proposes a local scheme for the fast detection of faults including HIFs in DC microgrid clusters. Both simulation and experimental results using a scaled DC microgrid cluster prototype and considering several scenarios (such as low impedance faults, HIFs, noise, overload, and bad calibration of sensors) demonstrate the successful and fast detection (less than 2 ms) of DC faults by the proposed method. Compared with other techniques, the proposed scheme presents its merits from the viewpoints of accuracy and speed.

KEYWORDS

power system faults, power system protection, relay protection

1 | INTRODUCTION

Due to the increasing penetration of DC loads and Renewable Energy Sources (RESs) in recent years, utilising DC systems could provide a more efficient power system due to the lack of skin effect, reduced power conversion stages, and lower line lengths [1]. With the recent developments in power electronic devices, hybrid energy storage, RESs, and smart homes, the DC microgrids have immerged as an essential element for future power systems. Besides, establishing DC microgrid clusters by interconnecting multiple DC microgrids has been proposed further to increase the reliability and power support of DC microgrids. Thus, each DC microgrid will be capable of sharing power with other DC microgrids. However, the lack of adequate standards and schemes for detecting faults in DC microgrids and DC microgrid clusters present a significant obstacle to the widespread implementation of DC microgrids [2].

The absence of phasor, frequency, and zero-crossing point in DC systems prevents the direct use of AC fault detection methods in DC systems. Therefore, differential, current rise rates, and overcurrent fault detection techniques are commonly implemented in DC microgrids [3, 4]. However, due to the high sensitivity of DC microgrid response to the impedance of fault, fault detection in such a system is challenging [5–7]. Moreover, the small change of current in the case of high impedance faults (HIFs) causes a more difficult situation in detecting faults. Also, it poses a challenge in setting overcurrent-based relays [8].

For achieving the fault detection capability in DC microgrid clusters, the implementation of a communication-based fault detection strategy is suggested in the literature [9–11]. However, the sensor noises, delay, and bad calibration prevent widespread communication-based fault detection techniques.

Power electronic converters are utilised for interfacing RESs and loads in DC microgrids. These converters have a limited overcurrent withstand for a short time, typically in the range of two or three times of normal current [12]. Furthermore, due to the short time constant of DC systems, the fault current rises rapidly during the fault. Therefore, faults in DC microgrid clusters should be detected within a few milliseconds before the fault's peak time.

Moreover, fault detection methods are categorised into communication-based and local strategies. The communication-based methods require the data of both sides of the protected line to detect the fault. On the other hand, the local fault detection schemes do not require any communication infrastructures, and local relays detect the fault events at the DC circuit breaker (C.B) place. Therefore, it can be immune to noise, delay, packet dropout, and additional costs [1] caused by communications.

Practically, due to the low damping of the DC fault current, the fault current will be discharged entirely within a few milliseconds. It significantly reduces the available fault data window and information; thus, the traditional fault detection techniques cannot be adapted during this rapid current discharge process. As aforementioned, one of the main challenges of fault detection is detecting HIFs. In some conditions, HIFs cannot change the current direction to the faulty point [13]. Consequently, change the current direction to the faulty point [13]. Consequently, the directional-based fault detection methods are ineffective when the fault current is lower than the normal working current. To solve this problem, the authors in [14] utilise the imposed fault current, as the differences of post and pre-fault currents, to detect faults in DC systems; however, it cannot provide sufficient sensitivity for HIF detection. Thus, in [15], HIF detection in low-voltage DC systems is suggested by using mathematical morphology. However, due to the high dependency of this method to fault current magnitude, the HIFs, for maximum detectable fault resistances, are detected within 1 s, which is not acceptable in many practical applications.

On the other hand, in traditional current-based fault detection methods, which use fault current magnitude, due to the rise time of the fault current, it takes several milliseconds to the fault current exceeds the threshold index. On the other hand, during HIFs, the fault current magnitude will not change dramatically; therefore, using only fault current magnitude is not a sufficient way, in terms of HIF detectability and fault detection time [6].

In recent years, growing digital signal processing applications on fault detection methods in DC microgrids have been studied [16–18]. Wavelet transform (WT) and Fast Fourier transform (FFT) are widely utilised techniques on time-domain and frequency analyses. FFT-based fault detection technique for a voltage source converter-based DC system has been proposed in [16]. The drawback of FFT is limited time-frequency resolution, in which low frequencies are depicted hardly with short windows. In contrast, high frequencies are poorly localised in long data windows.

On the other hand, the WT-based method decomposes signals into specific time-frequency resolution. In [17], a fault detection method in DC microgrid has been studied by the energy level and WT percentage. Furthermore, the improved WT has been used in [18] to detect a fault in DC microgrids with high integration of PV systems. However, the WT technique is vulnerable to noise and network disturbances [19].

Another effective signal processing technique recently used in different power system applications is empirical mode decomposition (EMD). In summary, EMD has been used previously for the determination of hybrid energy storage system capacity [20], islanding detection [21], power imbalance [22], and inverter's harmonics identification [23]. In [24], a differential fault detection method is suggested for AC microgrids protection, which uses EMD for detecting faults. However, it cannot detect HIFs and is high sensitivity to communication links. Most existing signal-processing-based fault detection methods are for AC systems, and there is still no accurate and fast fault detection scheme of DC microgrid clusters. Furthermore, most DC microgrid protection schemes rely on communication links, which causes several practical issues. Furthermore, the existing signal-processing-based DC microgrid fault detection techniques [9] require more improvements to address vulnerability to noise, reduce fault detection time, and include the HIF detection function.

Furthermore, the Hilbert transform (HT) is a time-frequency signal processing method. It is one of the fastest high-frequency fault detection methods and has been implemented in different applications, especially on motor fault detections [25–27]. In [26], the current envelope of the stator is utilised by HT for fault detection inside of motors. This envelope determines information of low-frequency components to provide a fast and accurate fault detection technique.

To address the research gaps mentioned above, in this work, an EMD-based fault detection scheme is proposed for DC microgrid clusters. Considering the transient behaviour of fault current during both high and low impedance faults (LIF), a localised method for multiple faults separation and detection in DC microgrid clusters is developed based on a combination of EMD and HT techniques. Therefore, the fault current transients are analysed and detected quickly by using the instantaneous frequency and the time-frequency-magnitude spectrum analysis. This signal analysis scheme can be used for detecting faults in tie-lines by using local sensors. The proposed method provides accurate and fast fault detection functions, compared to the existing fault detection methods. The proposed technique does not use communication links; therefore, delay, cost, and vulnerability to noise are minimised.

The remainder of this paper is organised as follows: Section 2 explains the architecture of the studied DC microgrid cluster. Section 3 describes the EMD and HT techniques and the detailed structure of the proposed fault detection method. Section 4 presents the simulation and experimental results and discusses the performance of the proposed fault detection technique. Finally, Section 5 concludes this paper.

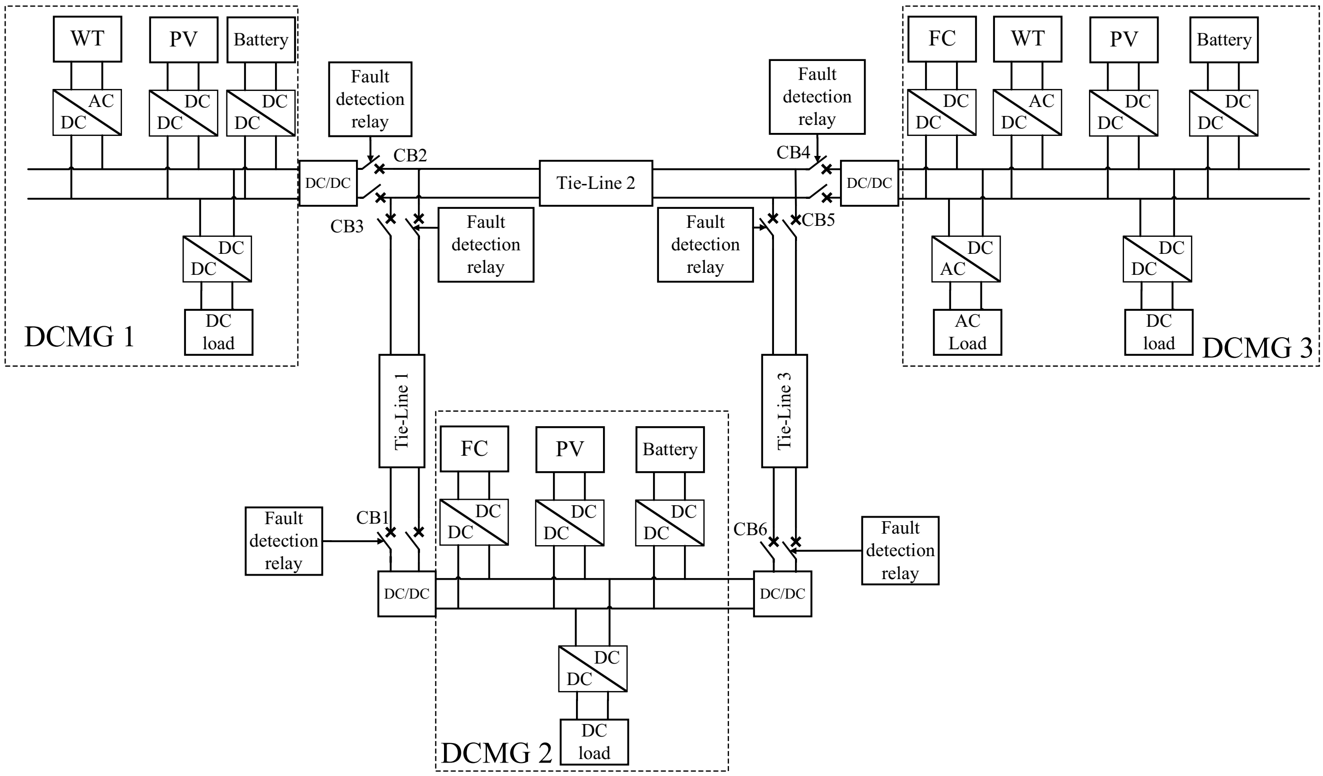

FIGURE 1 Configuration of the DC microgrid cluster

2 | STRUCTURE OF DC MICROGRID CLUSTERS

The general structure of an RES-based DC microgrid cluster is depicted in Figure 1, which includes three DC microgrids: DCMG 1, DCMG 2, and DCMG 3. The RESs are connected to the main DC bus by DC/DC and AC/DC converters, and due to the different voltage levels between DC microgrids, each DC microgrid is connected to the neighbour DC microgrid by a DC/DC converter. Therefore, this system can provide mutual power support among the cluster system. Each DC microgrid has different types of components, DCMG 1 is a combination of WG units, PV, battery, and DC loads, DCMG 2 consists of battery, fuel cell (FC), photovoltaic (PV), and DC loads, and DC MG 3 has PV, FC, wind generation (WG), battery, and DC and AC loads.

The DC microgrid cluster's protection layer is a combination of the DC C.B, fault detection relays, and measurement units.

From the protection point of view, all DC microgrids inject fault current to the faulty point during the fault at the tie-line between DC microgrids. Therefore, with the high penetration of RESs and DC/DC converters in these systems, the magnitude of fault current has a wide range, depending on the fault resistance. Because both sides of each tie-line are connected to a DC/DC converter, the capacitor of converters injects a high-rise current into the faulty point during the fault. Consequently, the fault current in DC tie-lines can be defined by (1) [28]

$$I_{fault} = -\frac{I_0\omega_0}{\omega}e^{-\alpha t}\sin(\omega t-\beta)+\frac{V_0}{\omega L}e^{-\alpha t}\sin\omega t$$

$$\begin{cases}\alpha = R/2L\\ \omega=\sqrt{1/LC-\alpha^2}\\ \omega_0=\sqrt{\alpha^2+\omega^2}\\ \beta=\arctan(\omega/\alpha)\end{cases} \tag{1}$$

As observed from (1), the fault current amplitude in DC systems depends on initial voltage and current, and fault resistance. Therefore, it is pivotal to detect fault fast in tie-lines of DC microgrid clusters. These issues cause difficulties for fault detection relays in terms of determining a current magnitude threshold to detect the fault. As mentioned above, the HIFs cause a small change in current magnitude; therefore, these types of faults cannot be seen by traditional relays and then cause damages to power electronic devices.

3 | HYBRID EMD AND HT METHOD

In this work, the hybrid EMD and HT method is proposed as the signal processing tool to detect HIF with local current sensors. This hybridisation is appropriate for analysing non-stationary and non-linear signal waveforms. These signal spectrums are usually composed by complex oscillation modes. Therefore, the instantaneous frequency derived by using HT upon the signal spectrum will be meaningless. However, the EMD timescale is based on the local features of the signal and decomposes a complicated signal waveform into different IMFs, and each IMF has a different physical explanation of the instantaneous frequency. Utilising HT to IMFs will get instantaneous amplitude and frequency and construct the signal spectrum distribution, which detects underlying faults.

3.1 | Empirical mode decomposition

All oscillation events generally make a transient signal. Inherent features can be retrieved from non-sinusoidal signals by determining the lower and higher envelopes of it, as shown in Figure 2. Then, both envelopes are averaged to obtain a mean oscillation signal. This signal is an estimation of the first oscillation component. The second component is calculated by subtraction of the first component from the original signal. These are the principles of EMD [29]. Therefore, any non-sinusoidal transient signal is divided into many different fluctuating components estimated by EMD [30]. The steps of the EMD tool are introduced as follows:

1. Determine the local extrema and connect them to make the lower and upper envelopes.
2. Calculate the m_1.
3. Obtain the h_1 by the difference between the given signal and m_1 as

$$x(t) - m_1 = h_1 \tag{2}$$

4. Repeat steps 1–3 with h_1 to calculate h_{11}, where is a principle inherent mode function as

$$h_1 - m_{11} = h_{11} \tag{3}$$

5. If h_{11} satisfies the IMF conditions, the integral of IMF should be zero, and the numbers of extrema and zero-crossing points should be equal, then the first IMF is calculated, else the steps are repeated, and after n times the h_{1n} is

$$h_{1(n-1)} - m_{1(n-1)} = h_{1n} \tag{4}$$

6. h_{1n} is the first IMF, then

$$r_1 = x(t) - h_{1n} \tag{5}$$

7. Repeat steps 1–5 to calculate the second IMF.
8. Repeat steps 1–6 to calculate IMFs of the original signal.

An online EMD is essential to detect faults in DC microgrid clusters in this research. Based on the EMD technique, the input signal is a function of time, and the statics are given as

$$s(t_1), s(t_2), \ldots, s(t_m) \tag{6}$$

Windows are considered to store data, and each window has a length of l, and it is given as

$$\begin{matrix} \text{section 1: } s(t_1), s(t_2), \ldots, s(t_l) \\ \text{section 2: } s(t_{l+1}), s(t_{l+2}), \ldots, s(t_{2l}) \end{matrix} \tag{7}$$

Therefore, the following aspects of the online application of the EMD algorithm should be considered.

In the standard algorithm [29], the subsequent points are performed $k \times n$ times. This increases the computational burden, and the alternative sections should wait in windows until all data are finished. Therefore, this method is not appropriate.

By preserving the span of data noticeably, computation's burden is relieved due to the dependence on EMD on the statics span.

The window width should be selected based on the sampling rate to have efficient data samples in each window with a low burden time to ensure the fast operation of the fault detection method. If each window has x samples, the window width is chosen by $x/(\text{sampling rate})$.

3.2 | Hilbert transform

After obtaining IMFs for each window, the HT is applied to IMFs for computing the instantaneous magnitude and frequency. For each $c_i(\sigma)$, $H_i(t)$ can be obtained by

$$H_i(t) = \frac{1}{\pi} P \int_{-\infty}^{\infty} \frac{c_i(\sigma)}{t - \sigma} d\sigma \tag{8}$$

Usually, P is 1 [31]. This can be used to determine an analytical signal $z(t)$ as

$$z_i(t) = c_i(t) + jd_i(t) = a_i(t) e^{j\varphi_i(t)} \tag{9}$$

where

$$\begin{cases} a_i(t) = \sqrt{c_i^2(t) + d_i^2(t)} \\ \varphi_i(t) = \arctan\left(\dfrac{d_i(t)}{c_i(t)}\right) \end{cases} \tag{10}$$

Then, the instantaneous frequency is

$$\omega_i(t) = \frac{d\varphi_i(t)}{dt} \tag{11}$$

Thus, the value of the HT signal is calculated by

$$ht(t) = \mathrm{Re} \sum_{i=1}^{m} a_i(t) e^{j\int \omega_i(t) dt} \tag{12}$$

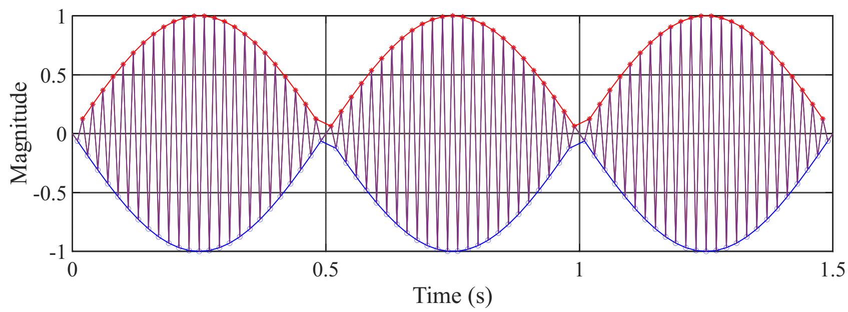

FIGURE 2 Lower and upper envelopes of a signal

This equation enables presenting the signal based on the instantaneous frequency and magnitude. Accordingly, the original signal could be shown by the sum of the IMFs and the sum of the HT magnitude. It could be noted that the HT works significantly for mono-component signals. However, most signals in practical applications are multi-components and have noise. Therefore, the HT will generate a spurious magnitude at a negative frequency. To solve this problem, the hybridisation of EMD and HT, due to the analysis of a series of IMFs, can avoid noise.

3.3 | Proposed fault detection scheme

The proposed fault detection scheme combines EMD and HT methods for implementing a local fault detection technique for DC microgrid clusters. In this scheme, EMD helps avoid noise and extract the features for detecting the fault, and HT helps to detect the HIFs and LIF by using IMFs and minimising the impact of fault resistance. Sensors measure the fault current at DC C.B places at the first stage. The sampling rate of sensors is an essential factor for selecting them. This application's suitable sampling rate is at least 10 kHz [1]. Due to the proposed method's local nature, the communication links between fault detection relays are eliminated; therefore, delay and noise are minimised. The installation place of fault detection relays is shown in Figure 1. Then, each line's current is analysed by a hybrid of EMD and HT in a fault detection relay. The first IMF, calculated by EMD, is observed during the fault, and the HT determines the frequency and amplitude by (12). The first IMF component from the data contains the highest oscillation frequencies found in the fault current signal. Therefore, first IMF is used for feature extraction in this scheme since most frequency content is present in this IMF and it will be sufficient for fault detection. The flowchart of the proposed method is depicted in Figure 3.

Despite the current amplitude-based methods, this method is immune to the variation of fault resistance due to the proposed method's frequency-based characteristic. Therefore, the HIF with a high value of fault resistance and low change in amplitude of fault current is detectable. The steps of the proposed technique are as follows:

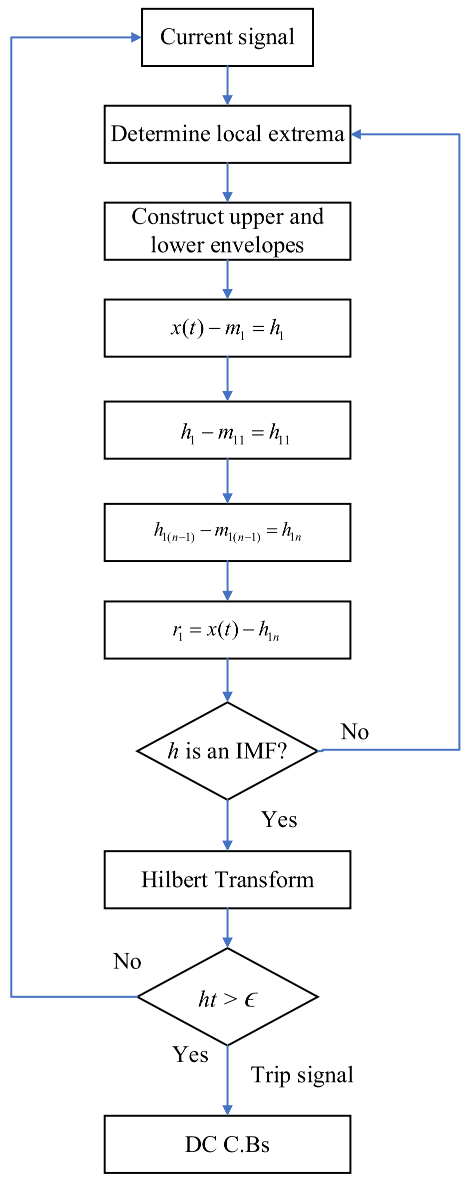

FIGURE 3 Flowchart of the proposed method

Step 1: Measuring the current by sensors at local places.

Step 2: Calculating the first IMF by EMD and analysing it by HT by fault detection relay.

Step 3: If the output value of fault detection is lower than a threshold ϵ, the operation mode of systems is on normal mode, else, the fault occurred.

Step 4: Send the trip signal to the DC C.B.

To avoid tripping during overloads, the value of the ϵ should be determined based on the worst case of overload. Here, the value of ϵ is selected on a case with 120% overload.

4 | SIMULATION AND EXPERIMENTAL RESULTS

This section represents the simulation and experimental results of the proposed fault detection scheme for DC microgrid clusters.

4.1 | Simulation results

In the simulation test, the case study of Figure 1 by system parameters of Table 1 is considered. The sampling rate is considered as 25 kHz, and local fault detection relays are installed at both ends of each line. Based on the overload conditions, in this work, for simulation tests, the threshold value is selected by $\epsilon = 0.001$. Therefore, in the under-study setup, the output value of the EMD/HT technique during a 120% overload, modified to the DC systems based on the NEC 705.12, at every fault detection relay location is determined. This output value is selected as the threshold of fault detection relays for detecting the fault. In any scenario, in which the output value of EMD/HT becomes higher than this value, the fault detection relay will send trip signals to C.Bs.

A fault at tie-line 1 with fault resistance of 0.01 Ω at $t = 0.3$ s has occurred. The fault current behaviour, IMF, and HT signals are presented in Figure 4. Fault current reaches the peak value after 20 ms, and the fault is detected within 0.6 ms. It shows that the fault is detected before the peak time, and it avoids any damages to power electronic devices because the thermal tolerant of power electronic devices defined by the value of I^2t, and isolating the fault before peak time causes de-energising the faulty section within the low value of I^2t. In Figures 5 and 6, the original fault current, IMF, and HT signals for a fault at tie-line 2 with R_f of 0.5 Ω and a fault at tie-line 3 with R_f of 20 Ω at $t = 0.3$ s are shown, respectively. In Figure 5, the fault is detected within 0.7 ms, and by increasing R_f to 20 Ω, the fault is detected within 2.2 ms, as shown in Figure 6. Therefore, the detection time of the HIF is also in an acceptable range. Also, as shown in Table 2, during other HIF scenarios, the proposed scheme's operation time is less than 2 ms, and it is significantly lower than the peak time of fault current. For LIFs, with R_f less than 2 Ω, the detection time is less than 1 ms.

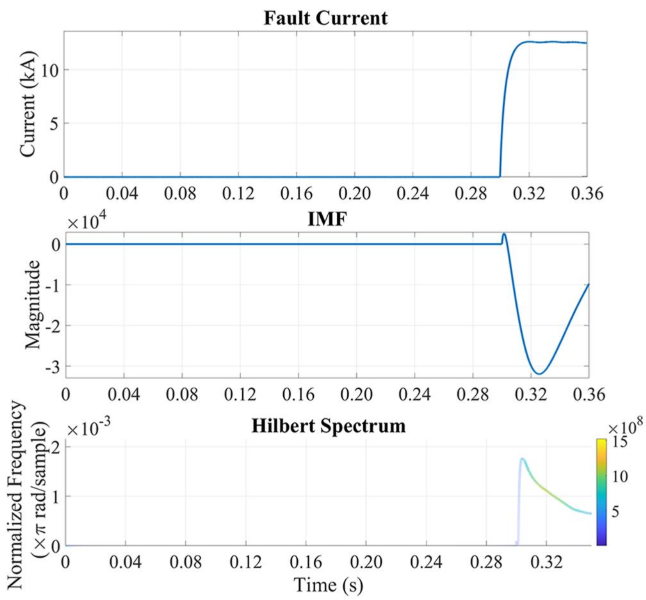

FIGURE 4 Fault current and detection signals for a fault at tie-line 1 with fault resistance of 0.01 Ω at $t = 0.3$ s

TABLE 1 System parameters of simulation case study

Component	Rating
Line lengths (km)	$Line_1 = 10$, $Line_2 = 10$, $Line_3 = 5$
Inductance and resistance	$R = 10$ mΩ/km, $L = 0.05$ mH/km
Nominal voltage	480 V
RESs in DC microgrids	DC microgrid$_1$: Fuel cell, WG, PV
	DC microgrid$_2$: Fuel cell, WG
	DC microgrid$_3$: WG, PV
FCs	100 kW, Ohmic loss per cell: 0.000328 Ω, number of cells: 1000
WGs	200 kW, reactance: 3.23 Ω
PVs	$V_{OC} = 64.2$ V, $I_{SC} = 5.96$ A, 25 series module, 66 parallel strings, series and parallel resistances for 1 module: 0.037 and 993 Ω, respectively.

Abbreviations: FC, fuel cell; PV, photovoltaic; RESs, Renewable Energy Sources; WG, wind generation.

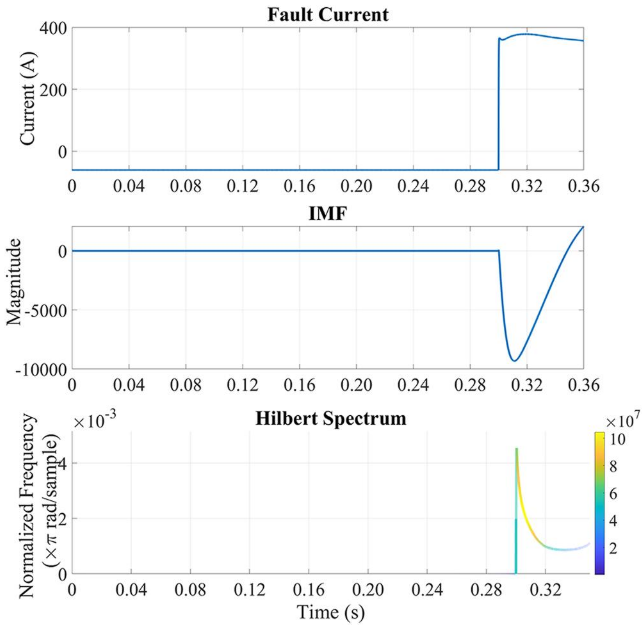

FIGURE 5 Fault current and detection signals for a fault at tie-line 2 with fault resistance of 0.5 Ω at $t = 0.3$ s

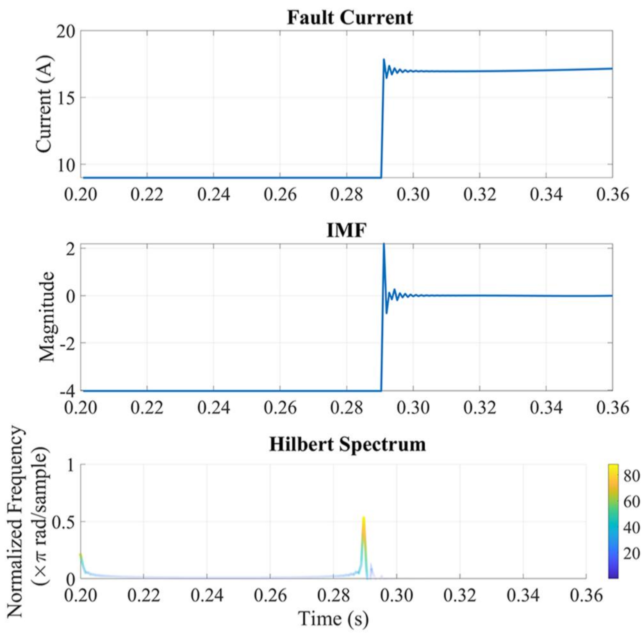

FIGURE 6 Fault current and detection signals for a fault at tie-line 3 with fault resistance of 20 Ω at $t = 0.3$ s

The proposed method's performance under noise and bad calibration and overload conditions is also investigated, and the results are shown in Figure 7. In this case, the bad calibration is modelled by a ±1% difference between the real current and the sensor's output. Moreover, in this case, a 10% overload at DCMG 2 is immediately connected. Furthermore, noise causes a ±2% variation in fault current values. The fault detection device's output signals prove the significant operation of the proposed method under different disturbances. Therefore, because the output signal's value is lower than ϵ, the fault detection device will not send the trip signal to the C.Bs. The proposed scheme's performance under different scenarios is summarised in Table 3. The comparison between Tables 2 and 3 shows that the noise only affects the detection time of HIFs with a value around 0.1 ms. Although bad calibration has a higher impact on both LIFs and HIFs, the proposed strategy's performance remains in an appropriate range of fault detection time.

TABLE 2 Fault detection time for different fault conditions

Fault location	R_f (Ω)	Detection time (ms)	Fault location	R_f (Ω)	Detection time (ms)
Line 1	0.01	0.6	Line 3	0.8	0.8
Line 1	0.4	0.7	Line 3	1.7	0.9
Line 1	3.7	1.1	Line 3	7.5	1.3
Line 1	10	1.7	Line 3	20	2.2
Line 2	0.05	0.6	DCMG1	0.2	0.6
Line 2	0.5	0.7	DCMG1	2	1.0
Line 2	5	1.2	DCMG2	2.5	1.1
Line 2	15	1.9	DCMG3	2	1.0

To compare the detailed results of the proposed work with existing methods, the comparison of the fault detection time of the proposed work and the mathematical morphology-based fault detection method [28] is presented in Table 4. As represented in Table 4, the fault detection speed of the proposed method is approximately 6 times higher than the mathematical morphology-based method.

4.2 | Experimental results

A DC experimental test system is built to create LIFs and HIFs, as shown in Figure 8. The DC system's voltage is 24 V. Converters' control, trip signal to solid-state circuit breakers, and fault detection scheme are performed by a dSPACE MicroLabBox controller. For dividing each line into several segments, each segment is modelled by resistance and inductance. The system has a rated DC bus voltage of 24 V DC, and each inductor is equivalent to a 400-m line, by the inductance and resistance of 0.01 mH and 0.16 Ω, respectively. The DC microgrid is equivalented by a DC power supply and connected to a DC/DC converter. The detailed parameters and specifications of the hardware setup are defined in Table 5.

The analysis results for LIFs, HIFs, and load change are shown in Figures 9 and 10. It should be noted that the LIFs and HIFs are categorised for faults with fault resistance lower and higher than 1 **Ω**, respectively. According to these figures, both LIFs and HIFs could be detected within 2 ms from the fault inception. As can be observed in Figure 9a, the fault current is increased to the maximum value within around 40 ms, and by using the proposed fault detection

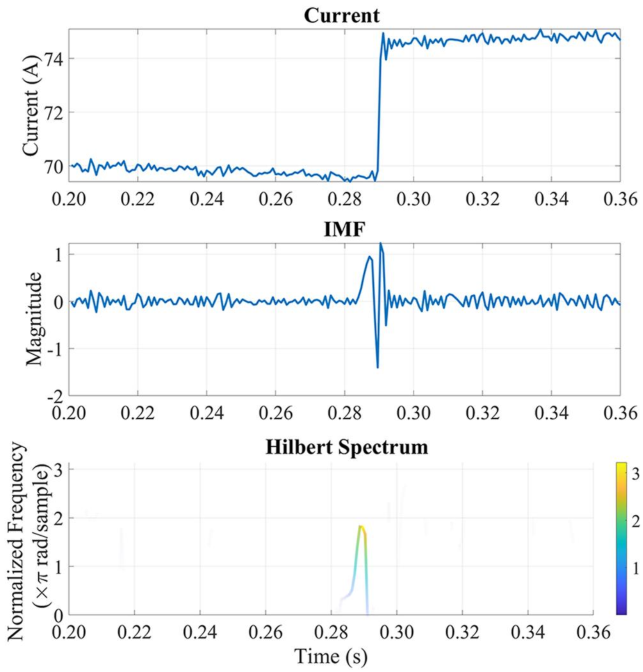

FIGURE 7 Current and detection signals under overload, noise, and bad calibration

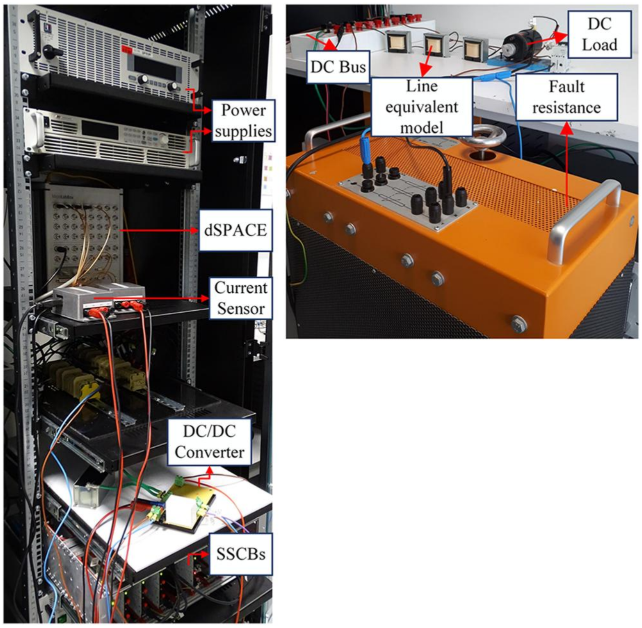

FIGURE 8 The experimental test setup

TABLE 3 Fault detection time for noise and bad calibration

Noise			Bad calibration		
Fault location	R_f (Ω)	Detection time (ms)	Fault location	R_f (Ω)	Detection time (ms)
Line 1	0.01	0.6	Line 1	0.01	0.7
Line 1	0.4	0.7	Line 1	0.4	0.9
Line 2	0.05	0.6	Line 2	0.05	0.6
Line 2	0.5	0.8	Line 2	0.5	1.6
Line 3	7.5	1.3	Line 3	7.5	1.9
Line 3	20	2.3	Line 3	20	2.8

TABLE 4 Fault detection performance of the proposed method and [28]

Fault location	R_f (Ω)	Detection time of proposed method (ms)	Detection time of [28] (ms)
Line 1	0.05	0.62	2.8
Line 1	0.40	0.70	3.2
Line 2	0.15	0.62	4.1
Line 2	0.10	0.61	3.7
Line 3	0.3	0.59	3.54
Line 3	0.1	0.57	4.98

method, as the results are provided in Figure 9b, the fault is detected within 1.5 ms, which is significantly lower than the peak time. As shown in Figure 10, the magnitude of the current increased instantly during overload conditions. However, the output signal of HT does not exceed the threshold; therefore, the fault detection device will not send an unnecessary trip signal to solid-state circuit breakers. The fault detection times of different fault resistance values and distances are shown in Table 6. The results prove the effectiveness of the proposed scheme under LIFs and HIFs in the hardware setup.

The computation complexity of the proposed method is measured by CPU time and memory. A computer with 3 -GHz i7-Core CPU, 8.0-GB RAM is used for the implementation of the proposed method. The computations for the analysis of fault signals by dSPACE require less than 1 ms, and memory around 10 MB. The complexity of EMD-based methods has been evaluated by counting the floating-point arithmetic operations in the main, extrema identification, and cubic spline procedures in [32]. It has shown that the time complexity of the EMD-based methods is equivalent to the traditional Fourier transform.

4.3 | Discussions

The simulation and experimental results show that the proposed fault detection system is validated by testing different scenarios and disturbances on a DC microgrid cluster. The results demonstrate that the developed fault detection scheme is fast and effective to detect faults in tie-lines and DC microgrids with resistances up to 20 Ω within 2 ms. This value of fault resistance is categorised as a HIF level, which is difficult or impossible to detect by other existing methods. Moreover, the operation time

TABLE 5 Parameters of hardware test setup

Component	Parameter
Line	Resistance = 0.4 Ω/km, Inductance = 25 mH/km
Power supply	Delta Elektronika SM 60–100
Motor	DC motor 10 W
Load	6.6 W DC resistive load
R_f	0–20 Ω
Measurement device	DPO 2024B, sampling rate 25 kHz, Tektronix TCP0020 AC/DC Current Probe
Threshold value	0.7

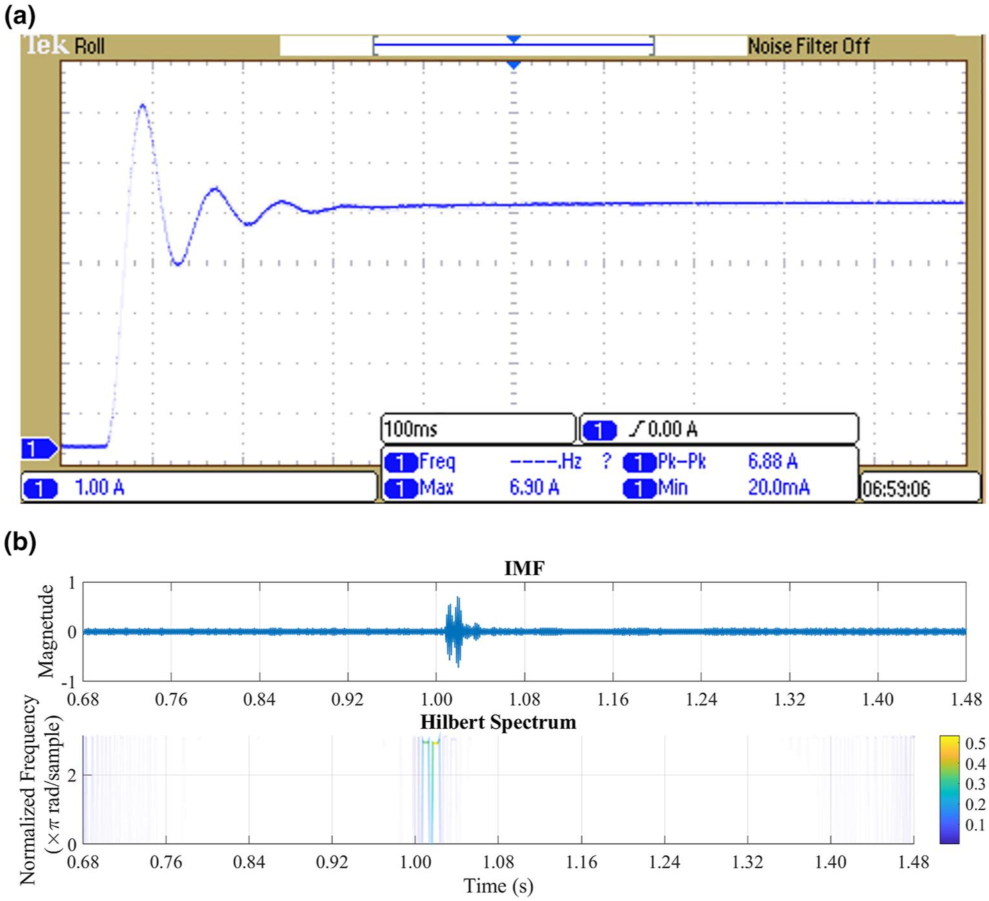

FIGURE 9 (a) The HIF current (b) HIF detection signals with $R_f = 9.5\ \Omega$ at 800 m

of 2 ms, as presented in Table 6, guarantees the safety of the whole DC microgrid cluster during faults. In addition, as shown in Table 3, noise and bad calibration cannot highly impact the performance of the proposed method, and as shown in Figure 7, the proposed fault detection scheme distinguishes between overloads and fault events, to ensure the lack of trip signal in overload events.

Furthermore, the implementation of the proposed fault detection scheme is communication-less; therefore, in addition to the lower cost compared to communication-based methods, issues such as delay and noise of communication links do not exist in the developed DC microgrid cluster protection system.

4.4 | Comparison

Table 7 presents the comparison of the proposed fault detection scheme with other existing fault detection methods in DC microgrids, that is, [9, 33–37].

As shown in Table 7, the proposed scheme's fault detection time is lower than other methods during both

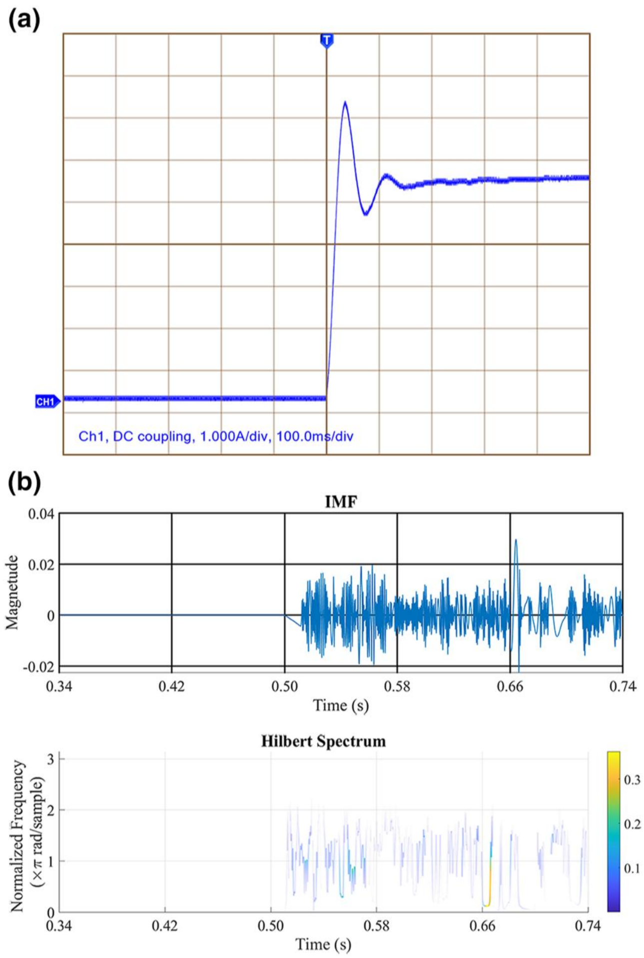

FIGURE 10 (a) The high impedance fault (HIF) current, (b) HIF detection signals with $R_f = 10.1\ \Omega$ at 400 m

TABLE 6 Fault detection performance in experimental tests

Fault location	R_f (Ω)	Detection time (ms)	Fault location	R_f (Ω)	Detection time (ms)
0 m	0.1	0.61	800 m	6.8	1.36
0 m	0.8	0.73	800 m	10.0	1.52
400 m	1.4	1.15	1200 m	15.5	1.83
400 m	2.7	1.21	1200 m	19.8	1.97

LIFs and HIFs. Unlike [9, 33], the proposed method is a local fault detection method, which avoids any noise and delay of communication links and additional cost of the communication system. In [34, 35], the local fault detection method can detect only faults with maximum R_f of 0.5 and 2 Ω, respectively, without any HIF detection function. The suggested method in [36] is a local HIF detection method. However, the fault detection time for HIFs in this method is 5 ms, which is much higher than that of the proposed method and is not short enough to protect very sensitive power electronic devices. In [4], the local fault detection method detects faults in 15 ms for a maximum R_f of 1.3 Ω. The suggested method in [37, 38] implements a fault detection method by k-means data description method and detects both LIF and HIFs without using any communication links up to 90 Ω within 13 ms, which shows a low fault detection speed.

The proposed scheme detects both LIFs and HIFs within 1.2 and 2.2 ms, respectively. The maximum tested R_f value in this scheme is 20 Ω, which is high enough to detect all HIFs.

TABLE 7 Summarising the existing fault location methods

Method	Fault detection time (ms)	Maximum fault resistance (Ω)	Communication link	Cost	Vulnerable to noise
[4]	15	1.3	Not required	Low	No
[9]	87	2	Required	High	Yes
[33]	2	2	Required	High	Yes
[34]	1.25	0.5	Not required	Low	No
[35]	4	2	Not required	Low	No
[36]	5	20	Not required	Low	No
[37]	13	90	Not required	Low	No
Proposed method	2	20	Not required	Low	No

5 | CONCLUSIONS

In this work, a novel local HIF fault detection scheme is proposed for DC microgrid clusters through hybridising EMD and HT methods. Due to the local structure of the proposed method, the current measurement of one side of the line segment can be used to extract the features of fault current, using EMD and HT as signal processing tools. The proposed method enabled accurate fault detection unaffected by fault resistance and overloaded even under noise and bad calibration in the sensors. Moreover, this strategy ensured fast fault detection within DC current peak time to avoid any damage to power electronic converters. The proposed scheme has very low implementation obstacles due to only requiring local current sensors without communication infrastructures. The effectiveness of the proposed scheme was validated by simulations and experiments under different scenarios and also by comparisons to other reported techniques. Therefore, the proposed method can be implemented in DC microgrid clusters with different structures.

NOMENCLATURE

RES renewable energy source
AC alternating current
DC direct current
HIF high impedance fault

LIF	low impedance fault
C.B	circuit breaker
WT	wavelet transform
FFT	fast Fourier transform
PV	photovoltaic
FC	fuel cell
WG	wind generation
EMD	empirical mode decomposition
HT	Hilbert transform
L	inductance of line
R	sum of fault resistance and line resistance
C	DC-link capacitor
I_0	initial value of the capacitor current
V_0	initial value of the capacitor voltage
m_1	mean value of the envelope
IMF	intrinsic mode function
h_1	parent signal
m_{11}	mean of h_1 upper and lower envelopes
r_1	original signal
$s(t)$	input signal
$s(t_m)$	mth sectioned point
$c_i(\sigma)$	time signal
$H_i(t)$	HT value,
P	singular integral principal value,
Re	real part,
$ht(t)$	Hilbert magnitude,
ϵ	threshold,
R_f	fault resistance

ACKNOWLEDGEMENT

This research received no external funding.

CONFLICT OF INTEREST

The authors declare no conflict of interest.

DATA AVAILABILITY STATEMENT

Data sharing is not applicable to this article as no datasets were generated or analysed during the current study.

ORCID

Navid Bayati https://orcid.org/0000-0001-9247-0840
Zhengyu Lin https://orcid.org/0000-0001-7733-2431

REFERENCES

1. Bayati, N, et al.: Local fault location in meshed DC microgrids based on parameter estimation technique. IEEE Syst. J. Early Access, 1–10 (2021)
2. Beheshtaein, S., et al.: Review on microgrids protection. IET Gener. Transm. Distrib. 13(6), 743–759 (2019)
3. Bayati, N, et al.: DC fault current analyzing, limiting, and clearing in DC microgrid clusters. Energies. 14(19), 6337 (2021)
4. Park, J.-D., et al.: DC ring-bus microgrid fault protection and identification of fault location. IEEE Trans. Power Deliv. 28(4), 2574–2584 (2013)
5. Som, S., Samantaray, S.R.: Efficient protection scheme for low-voltage DC micro-grid. IET Gener. Transm. Distrib. 12(13), 3322–3329 (2018)
6. Bayati, N., Hajizadeh, A., Soltani, M.: Protection in DC microgrids: a comparative review. IET Smart Grid. 1(3), 66–75 (2018)
7. Abdali, A., Mazlumi, K., Noroozian, R.: High-speed fault detection and location in DC microgrids systems using multi-criterion system and neural network. Appl. Soft Comput. 79, 341–353 (2019)
8. Bayati, N, et al.: A fuse saving scheme for DC microgrids with high penetration of renewable energy resources. IEEE Access. 8, 137407-–137417 (2020)
9. Dhar, S., Patnaik, R.K., Dash, P.K.: Fault detection and location of photovoltaic based DC microgrid using differential protection strategy. IEEE Trans. Smart Grid. 9(5), 4303–4312 (2018)
10. Shabani, A., Mazlumi, K.: Evaluation of a communication-assisted overcurrent protection scheme for photovoltaic-based DC microgrid. IEEE Trans. Smart Grid. 11(1), 429–439 (2020)
11. Dhar, S., Dash, P.K.: Differential current-based fault protection with adaptive threshold for multiple PV-based DC microgrid. IET Renew. Power Gener. 11(6), 778–790 (2017)
12. Kempkes, M., Roth, I., Gaudreau, M.: Solid-state circuit breakers for medium voltage DC power. In: 2011 IEEE Electric Ship Technologies Symposium, pp. 254–257. (2011)
13. Saleh, K.A., Hooshyar, A., El-Saadany, E.F.: Hybrid passive-overcurrent relay for detection of faults in low-voltage DC grids. IEEE Trans. Smart Grid. 8(3), 1129–1138 (2017)
14. Mohanty, R., Pradhan, A.K.: A superimposed current based unit protection scheme for DC microgrid. IEEE Trans. Smart Grid. 9(4), 3917–3919 (2018)
15. Oh, Y.S, et al.: Detection of high-impedance fault in low-voltage DC distribution system via mathematical morphology. J. Int. Council Electr. Eng. 6(1), 194–201 (2016)
16. Satpathi, K., et al.: Short-time Fourier transform based transient analysis of VSC interfaced point-to-point DC system. IEEE Trans. Ind. Electron. 65(5), 4080–4091 (2018)
17. Som, S., Samantaray, S.R.: Wavelet based fast fault detection in LVDC micro-grid. In: 2017 7th International Conference on Power Systems (ICPS), pp. 87–92. (2017)
18. Naik, J., Dhar, S., Dash, P.K.: Effective fault diagnosis and distance calculation for photovoltaic-based DC microgrid using adaptive EWT and kernel random vector functional link network. IET Gener. Transm. Distrib. 18 (2019)
19. Hong, Y.Y., Cabatac, M.T.: Fault detection, classification, and location by static switch in microgrids using wavelet transform and Taguchi-based artificial neural network. IEEE Syst. J. 14(2), 2725–35 (2019)
20. Hettiarachchi, H.W.D., et al.: Determination of hybrid energy storage system capacity based on empirical mode decomposition for a high PV penetrated standalone microgrid. In: 2018 Australasian Universities Power Engineering Conference (AUPEC), Auckland, New Zealand, pp. 1–6. (2018)
21. Shao, Z, et al.: Kriging empirical mode decomposition via support vector machine learning technique for autonomous operation diagnosing of CHP in microgrid. Appl. Therm. Eng. 145, 58–70 (2018)
22. Dedović, M.M., Avdaković, S.: A new approach for df/dt and active power imbalance in power system estimation using Huang's Empirical Mode decomposition. Int. J. Electr. Power Energy Syst. 110, 62–71 (2019)
23. Moradifar, A., Foroud, A.A., Fouladi, M.: Identification of multiple harmonic sources in power system containing inverter-based distribution generations using empirical mode decomposition. IET Gener. Transm. Distrib. 13(8), 1401–1413 (2019)
24. Gadanayak, D.A., Mallick, R.K.: Microgrid differential protection scheme using downsampling empirical mode decomposition and Teager energy operator. Elec. Power Syst. Res. 173, 173–182 (2019)
25. Ramu, S.K, et al.: Broken rotor bar fault detection using Hilbert transform and neural networks applied to direct torque control of induction motor drive. IET Power Electron. 13(15), 3328–3338 (2020)
26. Xu, B., et al.: Improvement of the Hilbert method via ESPRIT for detecting rotor fault in induction motors at low slip. IEEE Trans. Energy Convers. 28(1), 225–233 (2013)
27. Abd-el-Malek, M.B., Abdelsalam, A.K., Hassan, O.E.: Novel approach using Hilbert transform for multiple broken rotor bars fault location

detection for three phase induction motor. ISA Trans. 80, 439–457 (2018)
28. Bayati, N, et al.: Mathematical morphology-based local fault detection in DC microgrid clusters. Electr. Power Syst. Res. 192, 106981 (2021)
29. Lavopa, E., et al.: Real time estimation of fundamental frequency and harmonics for active shunt power filter in aircraft electrical systems. IEEE Trans. Ind. Electron. 56(8), 2875–2884 (2009)
30. Huang, N.E., et al.: The empirical mode decomposition and the Hilbert spectrum for nonlinear and non-stationary time series analysis. Proc. R. Soc. Lond. A. 454, 903–995
31. Kschischang, F.R.: The Hilbert transform, vol. 83, p. 277. University of Toronto (2006)
32. Wang, Y.-H., et al.: On the computational complexity of the empirical mode decomposition algorithm. Phys. Stat. Mech. Appl. 400, 159–167 (2014)
33. Mohanty, R., Pradhan, A.K.: Protection of smart DC microgrid with ring configuration using parameter estimation approach. IEEE Trans. Smart Grid. 9(6), 6328–6337 (2018)
34. Meghwani, A., Srivastava, S.C., Chakrabarti, S.: A non-unit protection scheme for DC microgrid based on local measurements. IEEE Trans. Power Deliv. 32(1), 172–181 (2017)
35. Yeap, M., et al.: Time and frequency domain fault detection in VSC interfaced experimental DC test system. IEEE Trans. Ind. Inf. 14(10), 4353–4364 (2018)
36. Saleh, K.A., Hooshyar, A., El-Saadany, E.F.: Hybrid passive-overcurrent relay for detection of faults in low-voltage DC grids. IEEE Trans. Smart Grid. 8(3), 1129–1138 (2017)
37. Farshad, M.: Detection and classification of internal faults in bipolar HVDC transmission lines based on K-means data description method. Int. J. Electr. Power Energy Syst. 104, 615–625 (2019)
38. Ran, X, et al.: A novel k-means clustering algorithm with a noise algorithm for capturing urban hotspots. Appl. Sci. 11(23), 11202 (2021)

How to cite this article: Bayati, N., et al.: EMD/HT-based local fault detection in DC microgrid clusters. IET Smart Grid. 5(3), 177–188 (2022). https://doi.org/10.1049/stg2.12060